Earth and Planetary Science Letters 515 (2019) 145–153

Contents lists available at ScienceDirect

Earth and Planetary Science Letters

www.elsevier.com/locate/epsl

Major shifts in nutrient and phytoplankton dynamics in the North Pacific Subtropical Gyre over the last 5000 years revealed by high-resolution proteinaceous deep-sea coral δ^{15}N and δ^{13}C records

Danielle S. Glynn [a,*], Kelton W. McMahon [a,b], Thomas P. Guilderson [a,c], Matthew D. McCarthy [a]

[a] Ocean Sciences Department, University of California, Santa Cruz, Santa Cruz, CA 95064, USA
[b] Graduate School of Oceanography, University of Rhode Island, Narragansett, RI 02882, USA
[c] Center for Accelerator Mass Spectrometry, Lawrence Livermore National Laboratory, Livermore, CA 94550, USA

ARTICLE INFO

Article history:
Received 9 August 2018
Received in revised form 6 March 2019
Accepted 9 March 2019
Available online xxxx
Editor: D. Vance

Keywords:
carbon
nitrogen
isotopes
paleoclimate
deep-sea coral
Holocene

ABSTRACT

The North Pacific Subtropical Gyre (NPSG) is the largest continuous ecosystem on Earth and is a critical component of global oceanic biogeochemical cycling and carbon sequestration. We report here multi-millennial-scale, sub-decadal-resolution records of bulk stable nitrogen (δ^{15}N) and carbon (δ^{13}C) isotope records from proteinaceous deep-sea corals. Data from three *Kulamanamana haumeaae* specimens from the main Hawaiian Islands extend the coral-based time-series back ~5000 yrs for the NPSG and bypass constraints of low resolution sediment cores in this oligotrophic ocean region. We interpret these records in terms of shifting biogeochemical cycles and plankton community structure, with a main goal of placing the extraordinarily rapid ecosystem biogeochemical changes documented by recent coral records during the Anthropocene in a context of broader Late-Holocene variability.

During intervals where new data overlaps with previous records, there is strong correspondence in isotope values, indicating that this older data represents a direct extension of Anthropocene records. These results reveal multiple large isotopic shifts in both δ^{15}N and δ^{13}C values similar to or larger in magnitude to those reported in the last 150 yrs. This shows that large fluctuations in the isotopic composition of export production in this region are not unique to the recent past, but have occurred multiple times through the Mid- to Late-Holocene. However, these earlier isotopic shifts occurred over much longer time intervals (~millennial vs. decadal timescales). Further, the δ^{15}N data confirm that the extremely low present day δ^{15}N values recorded by deep sea corals (~8‰) are unprecedented for the NPSG, at least within the past five millennia.

Together these records reveal centennial to millennial-scale oscillations in NPSG biogeochemical cycles. Further, these data also suggest a number of independent biogeochemical regimes during which δ^{15}N and δ^{13}C trends were synchronous (similar to recent coral records) or distinctly decoupled. We propose that phytoplankton species composition and nutrient source changes are the dominant mechanisms controlling the coupling and de-coupling of δ^{15}N and δ^{13}C values, likely primarily influenced by changing oceanographic conditions (e.g., stratification vs. entrainment). The decoupling observed in the past further suggests that oceanographic forcing and ecosystem responses controlling δ^{15}N and δ^{13}C values of export production have been substantially different earlier in the Holocene compared to mechanisms controlling the present day system.

1. Introduction

Modern subtropical gyres are characterized by low nutrient concentrations and low primary production, with biogeochemical cycles typically dominated by microbial loop dynamics (Karl, 1999). These oligotrophic gyre systems comprise around 60% of the global oceans and are critical components of the global marine biogeochemical balance (Karl, 1999). It is now recognized that aggregate open-ocean oligotrophic regions, due to their vast extent, contribute the bulk of marine productivity and account for a substantial amount of global ocean export (Karl et al., 1997; Martin et al., 1987).

The North Pacific Subtropical Gyre (NPSG) is the largest contiguous ecosystem on earth, and remote sensing indicates that it

* Corresponding author.
E-mail address: dglynn@ucsc.edu (D.S. Glynn).

https://doi.org/10.1016/j.epsl.2019.03.014
0012-821X/

is rapidly expanding (Polovina et al., 2008). In contrast to global trends of declining marine productivity, phytoplankton communities of the NPSG are increasing in both biomass and productivity (Boyce et al., 2010; Corno et al., 2007; Karl et al., 2001). This is due to changes in plankton community structure, which appear to be linked to the addition of new nutrient sources from expanding communities of nitrogen-fixing diazotrophs, selected for by increased stratification (Karl et al., 1997, 2001, 2011). As such, understanding how algal community structure and nutrient supply have responded to physical forcing in the past is critical to understanding future changes in the ecosystem dynamics of these critical open ocean systems. As part of the Hawaiian Ocean Time-Series (HOT) program, instrumental observations taken at Station ALOHA (22°45′N, 158°W) suggest that variability in physical and biological attributes of the NPSG are coupled to inter-annual climate variability superimposed upon longer term, basin-wide variability (Corno et al., 2007; Di Lorenzo et al., 2008). While much can be gained from detailed instrumental records at ALOHA and other time-series stations, the short timescale of these records is inadequate to understand the coupling of biogeochemical cycles to long term climate forcing. Further, the low sedimentation rate in oligotrophic regions, such as the NPSG, means the entire Holocene is recorded in ~10 cm of bioturbated sediments, leading at best to uncertain, low resolution sediment records.

Cosmopolitan deep-sea proteinaceous corals are unique biogenic archives that can provide centennial to millennial-scale records at sub-decadal resolution of past ocean conditions. These azooxanthellate corals are low-order consumers which feed on recently exported particulate organic matter (POM), and record the isotopic signatures of this food source into the accretionary growth layers of proteinaceous skeletons (Roark et al., 2009; Sherwood et al., 2014; McMahon et al., 2017). The horny proteinaceous skeleton is composed of a fibrillar protein framework (Ehrlich et al., 2006) that is resistant to degradation (Sherwood et al., 2006). The Hawaiian gold coral *Kulamanamana haumeaae*, a colonial zoanthid, is extraordinarily long-lived, thus providing a bioarchive on multi-millennial timescales for the NPSG region with average radial growth rates in the low tens of microns per year (Guilderson et al., 2013; Roark et al., 2009).

Previous deep-sea coral records from the NPSG Hawaiian Islands spanning the last ~1000 yrs have shown dramatic decreases in both nitrogen (δ^{15}N; Sherwood et al., 2014) and carbon (δ^{13}C; McMahon et al., 2015) isotopic values since the Little Ice Age (~1850 CE) by ~1.5‰ and ~1.2‰ for δ^{15}N and Suess-corrected δ^{13}C respectively. These data indicate that both δ^{15}N and δ^{13}C values of exported primary production have strongly decreased, commensurate with 20th century warming and gyre expansion. Sherwood et al. (2014) used a multi-proxy compound-specific stable isotope approach to show that the declining deep-sea coral δ^{15}N values were indicative of an increase in the relative contribution of nitrogen fixation supporting export production in the NPSG over the last 150 yrs. McMahon et al. (2015) then used a compound-specific stable isotope δ^{13}C fingerprinting approach to show a concurrent shift towards more N_2-fixing cyanobacteria in the phytoplankton community supporting export production over this time period, consistent with the conclusions of Sherwood and co-authors.

Together, these records indicate dramatic responses in both broad algal community structure and fundamental biogeochemical cycles to shifting climate states of the NPSG. Specifically, these data have suggested: 1) direct coupling in major changes of primary production δ^{15}N and δ^{13}C values over the last ~1000 yrs, 2) that present primary production δ^{15}N and δ^{13}C values are the lowest in at least a millennium, 3) the variability in δ^{15}N and δ^{13}C of export production is driven primarily by algal community structure shifts, and 4) that stratification may be a major driver for these changes in plankton community dynamics (Sherwood et al., 2014; McMahon et al., 2015). However, in order to assess these hypotheses within the broader context of the Holocene, longer records are required to better understand the potential drivers for recent variability and to potentially facilitate predictions of ecosystem responses to future change.

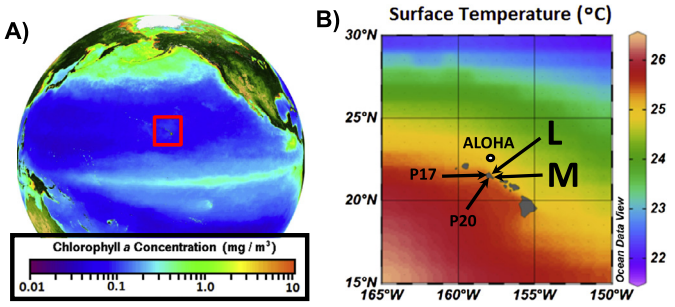

Fig. 1. Study location. A) SeaWIFS ocean color globe of chlorophyll during boreal summer with Hawaiian Islands squared in red. **B)** An annual SST (°C) map of Hawaii using World Ocean Atlas 1955–2015 annual data, with arrows pointing to the two coral collection locations on the eastern side of Oahu Island; L for Lanikai (this study), M for Makapu'u (Sherwood et al., 2014), and two sediment core locations P17 and P20 from Lee et al., 2001. Also shown is Station ALOHA from the HOTS program (open circle). (For interpretation of the colors in the figures, the reader is referred to the web version of this article.)

The main goal of this study was to determine if the dramatic changes documented in the last 150 yrs are in fact unique or if similar coupled δ^{15}N and δ^{13}C shifts are typical on millennial timescales. To answer these objectives, we report bulk stable nitrogen and carbon isotope records extending into the Mid-Holocene (~5000 yrs ago), from proteinaceous deep-sea coral specimens collected from offshore Oahu, Hawaii. Proteinaceous deep-sea coral skeletons' bulk δ^{15}N and δ^{13}C stable isotope values are a reliable proxy of baseline isotope dynamics represented by source and essential amino acid values (e.g., Schiff et al., 2014; Sherwood et al., 2014; McMahon et al., 2015, 2017). These new records are used to examine the stability of historical baselines in export production δ^{15}N and δ^{13}C values.

2. Materials and methods

Three sub-fossil *K. haumeaae* deep-sea coral samples were collected from ~400 m depth offshore of Lanikai on the island of Oahu, Hawaii (21°24.4′N, 157°38.6′W; Fig. 1). In the results and discussion below, we refer to individual specimens as Lanikai 1, 2, and 3 (L1, L2, and L3). Skeletons were washed with seawater then fresh water before being air-dried on deck. Cross section disks ~0.7 cm thick were cut from close to the basal attachment, polished, and mounted onto glass plates. A computerized Merchanteck micromill was used to isolate 2–3 mg of proteinaceous coral skeleton at 0.1 mm increments along radial transects from the outer edge to the center. The disk radius for L1, L2, and L3 were 17.5, 13.0, and 27.6 mm respectively. A subset of samples (1–2 mg each, 5–6 per coral) were acidified in 1N HCl for 20 hours under refrigerated conditions, filtered onto a 0.22 µM GFF which was then dried overnight at 45 °C before being scraped off into a tin capsule for EA analysis.

Bulk δ^{15}N and δ^{13}C analyses were conducted on ~0.3 mg raw material using a Carlo Erba 1108 elemental analyzer coupled to a ThermoFinningan Delta Plus XP isotope ratio mass spectrometer at the UCSC Stable Isotope Laboratory, following the lab's standard bulk stable isotope protocols (https://websites.pmc.ucsc.edu/~silab/EA_Protocol.php/). Results are reported in conventional per mil (‰) notation relative to air and VPDB standards for δ^{15}N and δ^{13}C, respectively. Laboratory error is 0.2‰ for both δ^{15}N and δ^{13}C, with duplicate coral analyses (n = 28) indicating 0.11‰ and 0.14‰ reproducibility for δ^{15}N and δ^{13}C, respectively. Coral C:N values

have a laboratory error of 0.1 as determined from repeated measurements of co-analyzed acetanilide.

Radiocarbon analyses were performed on 7–11 acid-pretreated sub-samples per specimen. Age models were determined for each specimen using Bacon, a Bayesian modeling approach (Blaauw and Christensen 2011), with Marine13 (Reimer et al., 2013), with more information available in supplemental materials. Isotopic regime shifts were detected using the methodology of Rodionov (2004), with a significance level of 0.1, cut off length of 10, and a Huber's weight parameter of 1. The regime shift program uses a sequential t-test to determine regimes and can detect shifts in both the mean level of fluctuations and the variance (Rodionov, 2004).

For comparison with published bulk sediment δ^{15}N records, marine sediment cores whose chronology were ^{14}C based were updated using Marine13 (Reimer et al., 2013; details in supplementary file). The δ^{15}N records from the NICOPP database (Tesdal et al., 2013) were differenced against the mean of each individual record for the last 6000 yrs, and datasets were combined to determine a regional, composite response. Sediment records were restricted to those that had more than two δ^{15}N sampling points in the last six millennia. Simple bivariate linear regressions were performed using JMP Pro® version 12 on both coral and sediment records to examine long-term trends and probabilities.

3. Results

3.1. Timescale and resolution

The 95% confidence interval for the individual age models averaged 98 ± 15 yrs (Fig. S1, Table S1). The L1 record (1510 to 220 CE) partially overlaps with the coral record from an adjacent location (M; Fig. 1B) in Sherwood et al. (2014) but extends the record by nearly 1000 yrs. L1 had an estimated average radial growth rate of 14 μm yr^{-1}, such that isotope samples averaged 7 yrs. The L2 coral spanned ~565 yrs (−20 to −580 CE) with a growth rate of 21 μm yr^{-1} and isotope data averaging 5 yrs. L3 was the oldest coral and spanned ~1420 yrs (−1540 to −2960 CE). L3 had an estimated growth rate of 19 μm yr^{-1}, with isotope data averaging 5 yrs.

3.2. Stable isotope results

Stable isotope data and C:N ratios as a function of radial distance and age are reported in Supplementary Table S2.

3.3. C:N ratio and acidification test as a screening tool

All samples from the live-collected Makapu'u coral skeleton in Sherwood et al. (2014) have an invariant C:N ratio of 2.86 ± 0.04, consistent with the 2.8–3.0 range previously reported for modern specimens (Druffel et al., 1995). A C:N of 2.86 ± 0.04 therefore represents the expected range for fresh coral skeletal material. While the average of all C:N values for the three fossil Lanikai corals are within error of this value (L1 2.89 ± 0.09, L2 2.90 ± 0.15, and L3 2.92 ± 0.06), there is also a persistent increase in C:N values for some samples in the outermost layers (Table S2). Comparison of acidified versus non-acidified duplicate samples from all three corals shows increases in both C:N and δ^{13}C values in only the outermost layers (Fig. S2, Table S2), with the distance of this effect increasing with time since the death of the colony and thus, seawater exposure time. The youngest fossil coral specimen (L1) showed no difference between acidified and non-acidified samples δ^{13}C values, however elevated C:N ratios in the outer 1.3 mm may suggest some skeletal degradation. For skeletons L2 and L3 the outer 1 mm δ^{13}C bulk values average + 0.8‰ more positive compared with acidified samples. Differences in δ^{13}C decline steadily

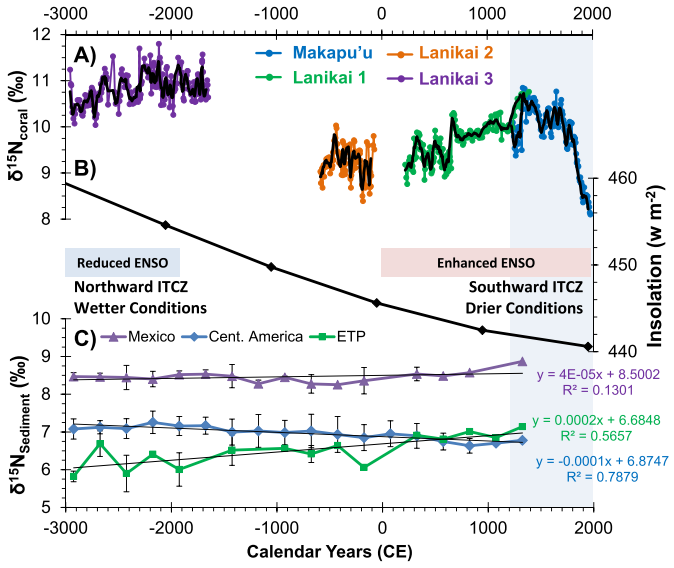

Fig. 2. Late Holocene bulk coral δ^{15}N records compared with selected climactic and sedimentary δ^{15}N records. **A)** Three new bulk coral δ^{15}N records from Lanikai (colors indicate coral; *see legend*); blue shading indicates previously published records (Makapu'u) from the same region. **B)** Mid-month insolation 15°N for July which is primarily driven by changes in solar precession cycles (Berger and Loutre, 1991). Also shaded are major ENSO periods where most proxy records agree (Lu et al., 2018). **C)** Data from bulk δ^{15}N sediment records from the North East Pacific binned by 250 yr time steps from 3 records from offshore Mexico (22 to 23°N), 5 off Central America (7 to 16°N), and 4 in the Eastern Tropical Pacific (ETP, 0 to 1°N). Data from the NICOPP database from Tesdal et al., 2013; see supplemental file for more information. Error bars indicate standard deviation.

toward the coral center, and both acidified vs. non-acidified values overlap within error in L2 by 2.2 mm and in L3 by 3.9 mm.

Based on these results and to be conservative in our interpretation, we have excluded samples from layers in which the C:N values or δ^{13}C values were influenced by acidification (Fig. S2, red shading). Further, throughout the entire remaining data set any sample for which C:N values were outside analytical error (±0.1) of the live collected Makapu'u coral values (<2.72 or >3.0) were excluded (Table S2). In the remaining data set (for which all samples had C/N values consistent with fresh coral skeletal material) when data for each coral is considered independently there remains a weak correlation between δ^{13}C and C:N ratio for two specimens (L1, $R^2 = 0.23$; L2, $R^2 = 0.12$). Therefore, while we cannot rule out the influence of diagenesis in our data set, the magnitude of potential δ^{13}C influence based on these regressions (~0.2‰ and ~0.1‰ of total δ^{13}C record variation, respectively) is very similar to analytical error relative to the larger coral δ^{13}C record trends and so should not influence the interpretations reported below.

3.4. Nitrogen stable isotopes

L1 δ^{15}N values overlap data from a specimen from nearby Makapu'u, presented in Sherwood et al. (2014), for nearly 170 yrs (Fig. 2A). L1 δ^{15}N values vary by ~2‰ from a low of 8.8‰ in 240 CE to a high of 10.8‰ in 1400 CE. There appears to be δ^{15}N oscillations around 9.4 ± 0.3‰ (n = 66) between 220 CE and 580 CE, followed by a large increase of ~1.2‰ from 660 CE to a high of 10.3‰ in 680 CE. δ^{15}N values then decline to an average of 9.9 ± 0.2‰ (710 CE and 1260 CE, n = 62) before increasing ~0.8‰ over the next two decades to overlap Makapu'u values.

The L2 coral (−70 to −580 CE) exhibits no clear secular trend but has substantial oscillations (range ~1.6‰) about the mean δ^{15}N value of 9.2 ± 0.3‰ (n = 101, Fig. 2A), similar to the values at the start of L1 300 yrs later. Regime detection (Fig. S3) notes periods of high δ^{15}N values during −420 to −450 CE (9.8 ± 0.2‰,

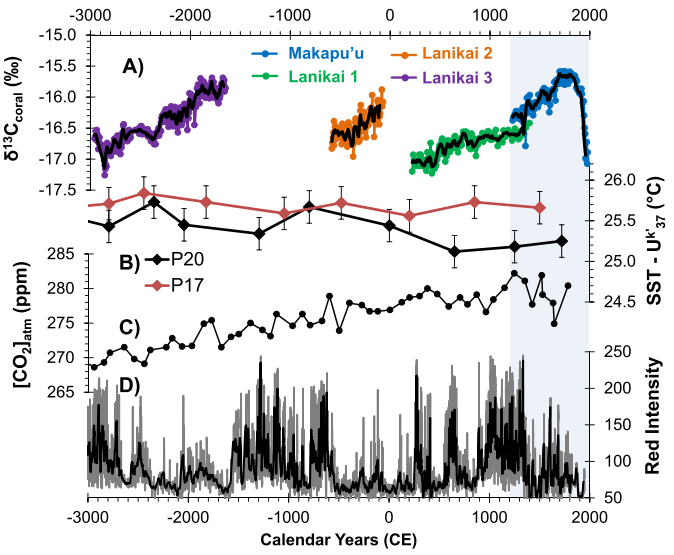

Fig. 3. Late Holocene bulk coral $\delta^{13}C$ records compared with selected climatic data, sedimentary and atmospheric $\delta^{13}C$ records. A) Bulk coral carbon isotope record, with blue shading depicting extent of previous coral records from the region, black lines representing a 5 point moving average. **B)** Alkenone SST records for the 2 sediment cores (P17, P20) collected near Oahu, Hawaii (Lee et al., 2001) believed to be representative of wintertime SST conditions in the NPSG. **C)** Atmospheric CO_2 concentration from Antarctic ice core records (Monnin et al., 2004). **D)** Red sediment color intensity record (gray), interpreted to be driven by El Niño Southern Oscillation with the black line designating a 20 yr moving average (Moy et al., 2002).

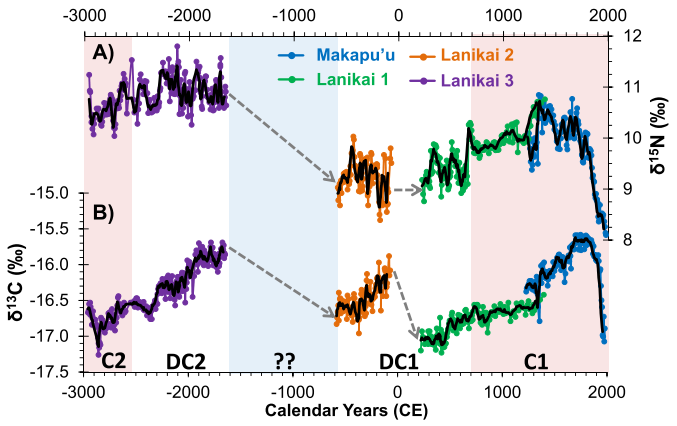

Fig. 4. Coupled vs. decoupled changes in $\delta^{15}N$ and $\delta^{13}C$ bulk isotope values of export production in NPSG through the Late-Holocene. Bulk nitrogen and carbon isotopic records from *K. haumeaae* (**A** and **B**; as presented in prior figures) are overlain to indicate distinct periods of coupling vs. decoupling in isotopic change. Unshaded period indicates where $\delta^{15}N$ and $\delta^{13}C$ are decoupled (DC1, DC2), while red shading indicates coupling as the isotope systems trend in the same direction (C1, C2), and blue shading is unknown (??). Grey dashed arrows indicate the hypothesized trend in isotope values during discontinuities in our current records while black lines designate the 5 point moving average.

n = 6) and −300 to −340 CE (9.5 ± 0.1‰, n = 10). The highest $\delta^{15}N$ value was 10.0‰ (−430 CE). Lower $\delta^{15}N$ values occurred between −190 and −100 CE (8.8 ± 0.4‰, n = 18), reaching 8.4‰ in −180 CE.

The Mid-Holocene L3 coral (−1650 to −2960 CE) has substantially more positive $\delta^{15}N$ values (10.8 ± 0.3‰, n = 225) compared to all of the Late-Holocene and near modern coral data (Fig. 2A). From −2940 to −2600 CE $\delta^{15}N$ increases 0.02‰ decade^{-1} (R^2 = 0.51, P < 0.0001) from 10.3‰ to 10.9‰, while reaching its lowest value of 10.0‰ in a brief excursion near −2720 CE.

3.5. Carbon isotope results

We observe a ∼2‰ total range in coral $\delta^{13}C$ values, with low $\delta^{13}C$ values very similar to present day occurring multiple times since the Mid-Holocene (in L1 ∼200 CE; in L2 ∼ −800 CE; in L3 ∼ −2800 CE, Fig. 3A). L1 $\delta^{13}C$ values begin low at −17.1 ± 0.1‰ (n = 43) between 220–460 CE, before increasing by ∼0.4‰ over the next few decades to an average of −16.7 ± 0.1‰ (480–1400 CE, n = 110). L1 coral $\delta^{13}C$ values overlap within 0.3‰ with previously published Makapu'u $\delta^{13}C$ records from 1230–1400 CE (McMahon et al., 2015).

The L2 $\delta^{13}C$ values range by ∼1‰ from −16.9‰ (−370 CE) to −15.8% (−80 CE) over the length of the ∼510 yr record (Fig. 3A). From a relatively stable 16.6 ± 0.1‰ (n = 27, −580 to −430 CE), $\delta^{13}C$ values increase towards the outer layers of the coral at a rate of 0.01‰ per decade (R^2 = 0.48, P < 0.0001). The L2 record indicates a large isotopic discontinuity in $\delta^{13}C$ values from the end of L2 to the more recent L1 $\delta^{13}C$ record.

The Mid-Holocene L3 record (−1650 to −2960 CE) is marked by a large and statistically significant, nearly unidirectional, $\delta^{13}C$ shift of ∼1.6‰ (∼0.01‰ decade^{-1}, R^2 = 0.84, p < 0.0001) with values ranging from −15.2‰ (−1540 CE) to −17.2‰ (−2860 CE) (Fig. 3A). Regime detection suggests this increase occurred between plateaus of more constant values (Fig. S3), from −16.6 ± 0.1‰ (−2680 to −2300 CE, n = 49), to −16.3 ± 0.1‰ (−2290 to −2080 CE, n = 41), before reaching a third plateau of −15.8 ± 0.1‰ (−1940 to −1630 CE, n = 64).

3.6. Coupling vs. decoupling of nitrogen and carbon isotope records

The combined isotope records show several distinct periods of coupling where $\delta^{13}C$ and $\delta^{15}N$ values trend similarly, corresponding closely to what has been observed in records from this region in the last millennium. However, equally common in the longer Holocene records are periods where $\delta^{13}C$ and $\delta^{15}N$ variability is decoupled, with little change in $\delta^{15}N$ while $\delta^{13}C$ changes dramatically. Unlike the most recent ∼1400 yrs with coupled $\delta^{13}C$ and $\delta^{15}N$, for more than a thousand years (−580 to 670 CE) $\delta^{13}C$ and $\delta^{15}N$ values are generally decoupled, suggesting a different regime than modern (Fig. 4, "DC1", representing L2 and part of L1). As noted previously, the $\delta^{15}N$ values throughout this period (−580 to 670 CE, including the gap between L1 and L2 records) remained relatively constant (mean of 9.3 ± 0.3‰), while in contrast the $\delta^{13}C$ values increased in L1 and L2 corals (from −430 to −70 CE and 250 to 670 CE), with an additional large decline in $\delta^{13}C$ values (∼1‰) required to connect values between these two records. Further back in the ∼1000 yr period between L3 and L2 (Fig. 4, "??"), the offset between coral records suggests an overall shift in both $\delta^{15}N$ and $\delta^{13}C$ to much lower values from past to present. The Mid-Holocene trends in $\delta^{13}C$ and $\delta^{15}N$ values are decoupled once again from −2550 to −1650 CE, with $\delta^{15}N$ values averaging 10.9 ± 0.3‰, while $\delta^{13}C$ values increase by ∼1.5‰. Finally, in the earliest part of this L3 records (−2950 to −2550 CE), both $\delta^{15}N$ and $\delta^{13}C$ values again trend in the same direction.

4. Discussion

4.1. Nitrogen isotopic records

The records exhibit a surprisingly wide range in $\delta^{15}N$ values of about 3.5‰, marked by several distinct regimes, with the most positive $\delta^{15}N$ values seen in the Mid-Holocene and lowest in the present day (Fig. 2). Using this new 5000 year $\delta^{15}N$ dataset for context, it is clear that the rate of the post-1850 decline (1.5‰ in 150 yrs) is unique. More common in the coral data are long periods of relative stability, with millennial-scale plateaus of similar $\delta^{15}N$ values in three intervals (from approximately −2960 to

−1650 CE, −580 to 660 CE, and from 660 to the 1800s; Fig. 2). While there are no direct coral data for the millennial-scale gap from −1530 to −580, the offset between L2 and L3 indicates that a ∼1.5‰ shift in $\delta^{15}N$ must have occurred in this period. However without more data it is not possible to determine if the shift in the $\delta^{15}N$ value of export production occurred rapidly, like the change in the last 150 yrs, or was more drawn out or variable over ∼1000 yrs (Fig. 2A).

Since nitrate is fully utilized on an annual scale in the NPSG, isotope mass balance requires that the overall $\delta^{15}N$ value of autotrophs represents an integrated signal of the $\delta^{15}N$ value of their nitrogen sources. Thus, gyre-based paleo-$\delta^{15}N$ records can be interpreted in terms of the relative balance of isotopically distinct nutrient sources supporting export production (e.g., Altabet, 2006; Dore et al., 2002; Sherwood et al., 2014). The large ∼3.5‰ variability in $\delta^{15}N$ values recorded in these corals could therefore be driven by either changing phytoplankton communities (i.e., relative importance of diazotroph N_2-fixation), and/or shifts in the source $\delta^{15}N$ value of advected nitrate. This latter aspect includes both the water mass being entrained during mixing due to changes in stratification as well as changing $\delta^{15}N_{NO_3}$ values sourced from the margins. Both situations could have been influenced by changes in water column stability and ocean-biogeochemistry dynamics.

In the NPSG near the Hawaiian islands nitrogen fixation leads to characteristically low $\delta^{15}N$ values (∼0‰) in the upper euphotic zone, while mesopelagic nitrate sources have much higher values (Dore et al., 2002; Casciotti et al., 2008). By assuming mass balance based on a two-component mixing model, with $\delta^{15}N_{N_2\text{-fix}} = 0‰$ and $\delta^{15}N_{NO_3} = 6.5‰$, and a sinking particulate bulk $\delta^{15}N$ value of 3.5 ± 0.2‰ at 300 m (Casciotti et al., 2008; Dore et al., 2002; Karl et al., 1997), around half (∼46%) of present-day exported production is supported by N_2 fixation. The amino acid phenylalanine $\delta^{15}N_{phe}$ values in Hawaiian proteinaceous corals have been used as a proxy for baseline nitrate and average 2.5 ± 0.3‰ over the late 20th and early 21st century (n = 7; Sherwood et al., 2014; McMahon et al., 2017), which implies a similar, albeit slightly higher (∼60%) fraction of export production supported by nitrogen fixation. As documented by Sherwood et al. (2014), there is a very strong 1:1 relationship ($R^2 = 0.77$) between bulk skeleton $\delta^{15}N$ and $\delta^{15}N_{phe}$ in *K. haumeaae*. Assuming that this 1:1 covariance is maintained in the Lanikai specimens, it is possible to directly transform (interpret) changes in bulk coral $\delta^{15}N$ variability into baseline variability.

Water column denitrification discriminates strongly against the heavier ^{15}N isotope, leaving seawater nitrate more positive in $\delta^{15}N$, and ocean circulation patterns can transport this isotopic signal from the Eastern Tropical Pacific throughout the Pacific (Altabet, 2006; Sigman et al., 2009). Analysis of North Pacific sediment records (n = 30) indicates an overall decline of ∼0.5‰ in bulk sediment $\delta^{15}N$ values since the Mid-Holocene (Figs. S4, S5). The decline in sedimentary $\delta^{15}N$ is assumed to reflect changes in source nitrate values and has been attributed to a decline in water column denitrification through the Holocene (Jia and Li, 2011 and references therein). However, a gradual ∼0.5‰ decline in North Pacific Ocean $\delta^{15}N_{NO_3}$ values clearly cannot be the primary driver of $\delta^{15}N$ values in our coral records, which exhibit significant variability in $\delta^{15}N$ values rather than a monotonic change. There is also little variability in sedimentary $\delta^{15}N$ values from source regions of the Eastern Pacific that intersect water-masses (isopycnals) ventilating the NPSG interior (Fig. 2C), which corresponds to variability in $\delta^{15}N$ export production as reconstructed by coral data. We are thus left with two potential mechanisms that drive the variability we observe. The first is a change in plankton community structure with variable importance of nitrogen fixing diazotrophs and the second is a change in the source of water being entrained into the mixed layer that provides nitrate to the NPSG. It is likely that the physical forcing for these two aspects is related: a more stratified ocean has diminished input from deeper water masses and could provide an expanded niche for diazotrophs (Karl et al., 2001; McMahon et al., 2015).

Mid-Holocene $\delta^{15}N$ values from the L3 specimen average 10.8‰ with sustained positive values in excess of 11‰. Within the context of the modern endmember model previously discussed, a value of 11‰ implies that ∼80% of the export production is supported by subsurface nitrate (i.e., only ∼20% supported by nitrogen fixation). By −580 CE, the NPSG contribution of N_2-fixation to export production is close to equal with the contribution of subsurface nitrate. By the beginning of the Little Ice Age (∼1450 CE), a return to production supported more by nitrate (∼70%) than nitrogen fixation (∼30%) appears likely. The value of entrained nitrate could be altered if there were 1) simply a higher concentration of NO_3^- sourced from similar present-day depth, 2) more positive $\delta^{15}N_{NO_3}$ entrained from deeper isopycnals, or 3) a different source origin. Deepening of the mixed-layer due to cooling and/or more frequent storm events (windiness) is an obvious mechanism to reduce stratification and increase the vertical flux of NO_3^- into the mixed-layer. In the modern NPSG, stratification is the most common underlying driver associated with shifts in diazotroph communities and rates of nitrogen fixation (Karl et al., 2001). Increased rates of N_2-fixation with abundant populations of *Trichodesmium* have been found to occur during the El Niño warm phase of El Niño Southern Oscillation (ENSO; Karl et al., 1995; Corno et al., 2007) when persistent subsidence leads to decreases in cloud cover, rainfall, and storminess in the Hawaiian Islands (Diaz and Giambelluca, 2012 and references within). A coupling of warm sea surface temperatures and increased stratification is likely associated with less cloudiness and reduced storminess, which should correspond to lower $\delta^{15}N$ values. Thus, on millennial timescales, the balance of nitrogen supporting export production likely reflects the large-scale circulation patterns associated with coupled ocean-atmosphere dynamics which follows summer insolation (Fig. 2B), affecting the descending limb of the Hadley Cell, which can impact ENSO and the migration of the Intertropical Convergence Zone (ITCZ, Clement et al., 2000; Schneider et al., 2014; Lu et al., 2018).

Solar forcing influences the position of the ITCZ by modulating its latitudinal extent (Clement et al., 2000; Schneider et al., 2014; Lu et al., 2018), which can influence NPSG surface ocean currents. Sediment $\delta^{15}N$ varies by latitude, with values ∼2.5‰ more positive offshore of Mexico in comparison to the equator (Fig. 2C). A southward ITCZ is expected to enhance equatorial upwelling (Schneider et al., 2014) and may impact the $\delta^{15}N$ of gyre waters by changing the source region of nitrate. When the ITCZ is located more southward such as during the Late-Holocene, water advects from lower latitudes in the Eastern Tropical Pacific which have comparatively more negative $\delta^{15}N$ values than higher latitudes (Fig. 2C). During the Mid-Holocene, a northward ITCZ may transport waters from latitudes with more positive nitrate $\delta^{15}N$ values. Future work modeling nitrate advection may help determine the contribution of nitrogen fixation versus a change in the source water impacting these coral isotopes.

4.2. Carbon isotopic records

The ∼2‰ range in coral $\delta^{13}C$ values across our 5000 year record also appear to occur within a number of discrete cycles, with low $\delta^{13}C$ values similar to present day having occurred multiple times since the Mid-Holocene (in L1 ∼ 200 CE; in L2 ∼ −800 CE; in L3 ∼ −2800 CE, Fig. 3A). Bulk coral $\delta^{13}C$ values have a strong, positive relationship with essential amino acid $\delta^{13}C$ values in *K. haumeaae*, particularly the $\delta^{13}C$ value of phenylalanine ($R^2 = 0.69$, McMahon et al., 2015), which indicates that most bulk

$\delta^{13}C$ variability can be tied to changes in the source carbon at the base of the food web. However, it should be noted that variations in bulk $\delta^{13}C$ values are typically muted in magnitude compared to the $\delta^{13}C$ signal from essential amino acids (Schiff et al., 2014; McMahon et al., 2015), thus suggesting bulk coral $\delta^{13}C$ records may underestimate the full extent of variability in baseline export changes.

There are multiple factors influencing planktonic $\delta^{13}C$ values in the marine environment, but on long timescales the dominant controls include SST, ambient CO_2 (aq.) concentrations, the $\delta^{13}C$ of dissolved organic carbon (DIC), and taxon-specific fractionation values (ε_f) (Rau et al., 1996; Young et al., 2013; McMahon et al., 2015, Table S3). Given that these factors can be inter-linked, definitively assigning causes to past changes in export production $\delta^{13}C$ values is challenging. Increased CO_2 availability, whether through increased atmospheric CO_2 concentrations or increases in [DIC], generally results in decreased phytoplankton $\delta^{13}C$ values and a greater isotopic discrimination between the phytoplankton and source CO_2 (Rau et al., 1989; Young et al., 2013). However, from the Mid-Holocene to the Little Ice Age, the concentration of CO_2 in the atmosphere has increased by only ~10 ppm, with little to no change in atmospheric $\delta^{13}C$ (Fig. 3C; Monnin et al., 2004), suggesting that the signal being recorded in these corals is not mainly due to pCO_2 change. The low sensitivity of plankton $\delta^{13}C$ to changes in pCO_2 (0.0003‰ ppm^{-1}; Young et al., 2013) would further indicate that atmospheric $\delta^{13}C$ value is not a main driving mechanism for the large changes in our coral records. Baseline changes in the $\delta^{13}C$ of DIC are also likely to be too small to be driving the trends in coral $\delta^{13}C$ (Quay and Stutsman, 2003; Monnin et al., 2004).

Laboratory and field experiments document that temperature exerts an important control on phytoplankton and exported organic matter $\delta^{13}C$ values (Table S3, and associated references). In general, warmer conditions contribute to more positive exported organic $\delta^{13}C$ values. Multiple approaches have attempted to quantify the effects of temperature on the $\delta^{13}C$ values of primary production, including estimates of the effect of temperature on fractionation factors in culture (ε_p; +0.12‰/°C), on natural phytoplankton $\delta^{13}C$ (+0.11–0.23‰/°C), and on suspended particulate organic carbon $\delta^{13}C$ (+0.41‰/°C) in natural ocean systems (Table S3). Mid- to Late-Holocene SST estimates using both the Modern Analog Technique and alkenone-SST relationships in sediment cores near Oahu indicate temperatures within 1°C of early 20th century data (Fig. 3B, Lee et al., 2001). These estimates are similar to higher resolution Northern Hemisphere reconstructions (e.g., Pei et al., 2017). A ≤1°C SST change would only account for ~0.4‰ or less of the 2‰ $\delta^{13}C$ variability, suggesting temperature alone is only partially responsible for the trends in coral $\delta^{13}C$.

Shifting plankton community composition, implicitly including size/morphology and growth rate, is the most likely explanation for the large changes in $\delta^{13}C$ values of our coral records over the last 5000 years. Different phytoplankton species have unique carbon isotope fractionations during photosynthesis (Laws et al., 1995; Rau et al., 1996), and thus a shifting phytoplankton community composition can be a major driver behind changes in $\delta^{13}C$ of export production over time (McMahon et al., 2015). Prokaryotic cyanobacteria (e.g., *Prochlorococcus*, *Synechococcus*) and picoeukaryotes are typically the dominant phytoplankton groups in open ocean regions like the NPSG (e.g., Karl et al., 2001), and of these, *Synechococcus* and picoeukaryotes are most strongly associated with carbon export in oligotrophic regions (Guidi et al., 2016). Picoeukaryotes are also larger than prokaryotes (cell diameters of 2.0 and 0.5 μm respectively) and this contributes to differences in their ecological performance as well as the extent of carbon fixation and export (Massana and Logares, 2013). Based on distinct isotopic fractionations associated with enzymatic, intracellular carbon fixation (ε_f; Laws et al., 1995; Scott et al., 2007), the differences between prokaryotic and eukaryotic contributions to exported organic matter manifest as differences in $\delta^{13}C$ values, where ~0.6‰ of $\delta^{13}C$ variability can be explained by a 1‰ shift in community fractionation ε_f (Table S3). More positive $\delta^{13}C$ values indicate higher relative contributions of eukaryotic phytoplankton, consistent with the well-known general trend that larger phytoplankton cells (e.g. diatoms) express more positive $\delta^{13}C$ values than small-celled nanoplankton (e.g., Laws et al., 1995; Popp et al., 1998).

Coral $\delta^{13}C$ values suggest centennial- to millennial-scale trends towards increasing eukaryotic contributions in exported production followed by hypothesized events (e.g. between L3 and L2) that reset the NPSG to be more prokaryotic-dominated. Picoeukaryotes are metabolically less flexible than prokaryotic organisms, perhaps causing them to be less resilient to environmental changes (Massana and Logares, 2013). Prokaryotic CO_2 fixers also outgrow and outperform eukaryotes in oligotrophic gyre ecosystems (Zubkov, 2014), which suggests that during periods of stratified, nutrient-limited conditions, prokaryotic organisms may dominate primary production and thus export production in the NPSG. The stability of the water column due to the frequency of ENSO events may influence community structure, with periods of low ENSO activity (e.g., ~3.5–5 kyrs ago) allowing for a long term community increase of eukaryotic organisms. This would result in the observed steadily increasing $\delta^{13}C$ values of coral L3, while periods of high ENSO activity (e.g. 1–2 kyrs ago and 3–4 kyrs ago; Moy et al., 2002, Fig. 3D) would correspond to a community consistently dominated by prokaryotes and low, stable $\delta^{13}C$ values (averaging -16.9 ± 0.2‰ from 200 to 1000 CE, Fig. 3). Shifts between smaller celled prokaryotes and larger picoeukaryotes can modulate the amount of organic matter exported to depth and may cause cascading effects on pelagic and benthic food webs (Finkel et al., 2010).

4.3. Coupling vs. decoupling of export production $\delta^{15}N$ and $\delta^{13}C$ values

Existing records from deep-sea corals from the NPSG in the last 1000 years have uniformly documented coupled changes in $\delta^{15}N$ and $\delta^{13}C$ values at the base of the food web, with authors hypothesizing that such shifts are linked to recent shifts in local/regional temperature and the ecosystem response derived from the dynamical oceanographic setting coincident with warmer surface temperatures (e.g., Sherwood et al., 2014; McMahon et al., 2015). Therefore the observation in the longer Holocene record that relative changes in $\delta^{15}N$ and $\delta^{13}C$ values of export production are often not coupled and trend in *opposite* directions was unexpected. The $\delta^{15}N$ and $\delta^{13}C$ data from these coral specimens clearly indicate two periods in which changes in $\delta^{15}N$ and $\delta^{13}C$ values are largely synchronous (moving in the same direction, with generally similar slopes), and two periods in which values appear decoupled (Fig. 4; *Results* 3.6). This suggests a more complex set of biogeochemical forcings on the longer timescale of these records.

In all coral records for the last millennium, the direct coupling between $\delta^{15}N$ and $\delta^{13}C$ shifts is one of the most striking overall features (Fig. 4). This observation supports the conclusion that regional plankton community changes are the underlying driver for changes observed in isotope records, primarily reflecting shifts between a more stable water column promoting oligotrophic and N_2-fixation conditions versus cooler periods with increased vertical mixing and entrainment (Sherwood et al., 2014; McMahon et al., 2015). Specifically, more recent warmer periods are characterized by more stratified and nutrient-poor conditions with enhanced nutrient recycling and fewer large eukaryotic cells (e.g., Chavez et al., 2011). Such conditions favor microbial-loop dominated systems characterized by lower $\delta^{13}C$ values. The enhanced N_2-fixation and nutrient recycling in such systems also

leads to lower $\delta^{15}N$ values, accounting for linked $\delta^{15}N$ and $\delta^{13}C$ changes. Conversely, higher nutrient environments are typified by faster growing, larger eukaryotic autotrophs supported by upwelled nitrate, leading to concurrent increases in both $\delta^{15}N$ and $\delta^{13}C$ primary production values.

The decoupling of $\delta^{15}N$ and $\delta^{13}C$ changes in earlier periods of this ~5000 year record suggest distinctly different local to basin-scale drivers for $\delta^{15}N$ and $\delta^{13}C$ values. While earlier data indicate several periods of coupled $\delta^{15}N$ and $\delta^{13}C$ change in the NPSG that appear to be analogues to the recent millennium, the distinct periods of coupling and decoupling must indicate different mechanisms are driving changes in primary production N and C cycles. The two periods of *decoupled* isotopic behavior (Fig. 4, DC1, DC2) occur when hemispheric temperatures may have been ~0.5° cooler than present (Pei et al., 2017) and proxy records suggest reduced ENSO climate variability (Lu et al., 2018; Moy et al., 2002). In contrast, the coupled period C1 includes the warmer Industrial Revolution and Medieval Climate Anomaly where proxy records agree on enhanced ENSO conditions (Lu et al., 2018 and references therein), and C2 occurs during enhanced ENSO activity periods as characterized by some proxy records (e.g. Moy et al., 2002, Fig. 3). One hypothesis for this apparently contrasted behavior is that coupling versus decoupling may be related to relative regional sea surface temperatures and stratification. Cooler periods of reduced ENSO variability are decoupled in $\delta^{15}N$ and $\delta^{13}C$ values, while warmer, enhanced ENSO periods are more consistently coupled. While speculative, this could be due to changing nutrient regimes. Generally warmer SSTs correspond to enhanced ocean stratification, shallower mixed layer depths, and a slowdown in gyre circulation. Under such oligotrophic conditions, phytoplankton communities may rely more heavily on the supply of N_2-fixed nitrate from localized diazotroph production, and community composition may shift towards prokaryotic, N_2-fixing organisms, perhaps causing a coupling in $\delta^{13}C$ and $\delta^{15}N$ values of export production. In contrast, there is both more mixing from depth and/or enhanced lateral advection of water from ocean margins during cooler, often windier, climatic periods (Sigman et al., 2009). The result is lower rates of N_2-fixation (Galbraith et al., 2004) and more nitrate with more positive $\delta^{15}N$ values possibly advected from higher latitudes of the Eastern Pacific (Fig. 2C). Thus, community composition changes may serve to shift $\delta^{13}C$ values, while the signal of advected $\delta^{15}N_{NO_3}$ and not N_2-fixation drives the $\delta^{15}N$ value of exported organic matter during periods of cooler SSTs, thus decoupling the $\delta^{13}C$ and $\delta^{15}N$ values. McMahon and coauthors (2015) support this idea, suggesting nitrate utilizing cyanobacteria dominate community composition over some periods while N_2-fixating cyanobacteria dominate over others during the most recent millennium. While this idea cannot be directly tested using bulk isotope analysis, further work could address it.

Lastly, spectral and wavelet analysis did not reveal consistent multi-decadal to centennial scale power and while the detected regimes did not often overlap in timing between $\delta^{15}N$ and $\delta^{13}C$ records most regimes (~60%) lasted between 30 and 90 yrs in duration (Fig. S3). We posit that the regime analysis confirms multi-decadal variability, but that there is more than one mechanistic forcing and ecosystem response influencing the $\delta^{13}C$ and $\delta^{15}N$ of export production, that are not always in sync with each other.

5. Conclusions

This study documents variability in export production $\delta^{15}N$ and $\delta^{13}C$ values for the Holocene NPSG, extending previously published records by approximately ~4000 yrs deeper into the Mid-Holocene. These new data reveal a dynamic biogeochemical system, in which substantial changes in $\delta^{15}N$ and $\delta^{13}C$ values of export production have been common on millennial timescales. Our records indicate that the natural isotopic range of production in the NPSG has varied by up to 3.5‰ for $\delta^{15}N$ values and 2‰ for $\delta^{13}C$ values over the last 5000 yrs. In particular, Mid-Holocene export production $\delta^{15}N$ values appear to have been substantially higher (by ~1.5 to 2‰) than in the Late-Holocene, and these longer records confirm that present day $\delta^{15}N$ values recorded in corals (~8‰) are the lowest in ~5000 yrs. In contrast, low $\delta^{13}C$ values similar to those recorded in modern corals (~−17‰) were reached during at least two other periods since the Mid-Holocene.

While these data clearly show periods of major change in both $\delta^{15}N$ and $\delta^{13}C$ values over the last 5000 yrs similar in magnitude to changes in the Anthropocene, past changes appear to have occurred over much longer (~millennial) timescales. In addition, these new records also indicate that distinct periods of coupled and decoupled $\delta^{15}N$ and $\delta^{13}C$ dynamics occurred in different periods throughout the Holocene. This in turn suggests a number of independent biogeochemical regimes over the last 5000 yrs. We hypothesize that these regimes are most likely linked to shifts in plankton community structure, possibly coupled with independently varying $\delta^{15}N$ values of nitrate in this region. The coupled $\delta^{15}N$ and $\delta^{13}C$ periods are similar to shifts observed in both NPSG instrumental records and also in more recent coral chronologies, likely explained by relative importance of nitrogen fixation and upper water stratification (McMahon et al., 2015; Sherwood et al., 2014). Periods in which $\delta^{13}C$ values change with no major shifts in $\delta^{15}N$ values imply changes in phytoplankton community structure without clear linkage to shifts in nutrient supply, potentially explained by relative abundance of non-nitrogen fixing prokaryotic autotrophs in this region (McMahon et al., 2015). However, to test these ideas more work will be necessary to identify the relative influence of baseline nutrient supply versus changes in autotrophic community structure.

Overall, the dynamism of Holocene biogeochemical systems revealed by this study strongly emphasizes the need to develop new proxies that can be used to determine past climate and environmental conditions at high resolution in the NPSG. Future work should include compound specific analysis of amino acids within coral archives to further constrain these hypotheses. Such information would allow researchers to directly examine if present microbial-loop dominated system of the NPSG has been constant or if variation in community structure has been responsible for isotopic variability of our records earlier in the Holocene. Further, this approach would allow for testing of the underlying assumption that average trophic structure of NPSG planktonic systems, which strongly influences the $\delta^{15}N$ value of export production, has remained constant through time. While data from Sherwood et al. (2014) indicated that average planktonic ecosystem trophic position has remained constant over the most recent millennium, it is not known if this also would hold true for earlier parts of this record, specifically during periods of $\delta^{13}C$ and $\delta^{15}N$ decoupling. Regardless, we show that while NPSG plankton and nutrient dynamics are highly variable over the last 5000 yrs, the modern Anthropocene regime remains unique in the magnitude and timing of changes in ecosystem dynamics in the context of Holocene variability.

Acknowledgements

None of this work would have been possible without the captain and crew of the RV *Ka'imikai-o-Kanaloa* and the pilots and engineers of the Hawaii Undersea Research Lab's Pisces IV and V. Sample collection was funded by NOAA/NURP and the National Geographic Society (7717-04). A portion of this work was performed under the auspices of the U.S. Department of Energy (DE-AC52-07NA27344). The majority of the work presented here was funded by the National Science Foundation (OCE 1061689).

D.S. Glynn was supported by the Eugene Cota-Robles Fellowship and National Science Foundation Graduate Research Fellowships Program (NSF-GRFP; 1339067). Further thanks go to D. Andreasen, C. Carney, R. Franks, and J. Schiff for laboratory assistance and training. We thank two anonymous reviewers for critical and constructive comments on the initial manuscript submission.

Appendix A. Supplementary material

Supplementary material related to this article can be found online at https://doi.org/10.1016/j.epsl.2019.03.014.

References

Altabet, M.A., 2006. Isotopic tracers of the marine nitrogen cycle: present and past. In: The Handbook of Enviromental Chemistry, vol. 2, pp. 251–293.

Berger, A., Loutre, M.F., 1991. Insolation values for the climate of the last 10 million years. Quat. Sci. Rev. 10 (4), 297–317. https://doi.org/10.1016/0277-3791(91)90033-Q.

Blaauw, M., Christen, J.A., 2011. Flexible paleoclimate age-depth models using an autoregressive gamma process. Bayesian Anal. 6, 457–474. https://doi.org/10.1214/11-BA618.

Boyce, D.G., Lewis, M.R., Worm, B., 2010. Global phytoplankton decline over the past century. Nature 466, 591–596. https://doi.org/10.1038/nature09268.

Casciotti, K.L., Trull, T.W., Glover, D.M., Davies, D., 2008. Constraints on nitrogen cycling at the subtropical North Pacific Station ALOHA from isotopic measurements of nitrate and particulate nitrogen. Deep-Sea Res., Part 2, Top. Stud. Oceanogr. 55, 1661–1672. https://doi.org/10.1016/j.dsr2.2008.04.017.

Chavez, F.P., Messié, M., Pennington, J.T., 2011. Marine primary production in relation to climate variability and change. Annu. Rev. Mar. Sci. 3, 227–260. https://doi.org/10.1146/annurev.marine.010908.163917.

Clement, A.C., Seager, R., Cane, M.A., 2000. Suppression of El Niño during the Mid-Holocene by changes in the Earth's orbit. Paleoceanography 15, 731–777. https://doi.org/10.1029/1999PA000466.

Corno, G., Karl, D.M., Church, M.J., Letelier, R.M., Lukas, R., Bidigare, R.R., Abbott, M.R., 2007. Impact of climate forcing on ecosystem processes in the North Pacific Subtropical Gyre. J. Geophys. Res. 112, 1–14. https://doi.org/10.1029/2006JC003730.

Di Lorenzo, E., Schneider, N., Cobb, K.M., Franks, P.J.S., Chhak, K., Miller, J., McWilliams, J.C., Bograd, S.J., Arango, H., Curchitser, E., Powell, T.M., Rivière, P., 2008. North Pacific Gyre Oscillation links ocean climate and ecosystem change. Geophys. Res. Lett. 35, 2–7. https://doi.org/10.1029/2007GL032838.

Diaz, H.F., Giambelluca, T.W., 2012. Changes in atmospheric circulation patterns associated with high and low rainfall regimes in the Hawaiian Islands region on multiple time scales. Glob. Planet. Change 98–99, 97–108. https://doi.org/10.1016/j.gloplacha.2012.08.011.

Dore, J.E., Brum, J.R., Tupas, L.M., Karl, D.M., 2002. Seasonal and interannual variability in sources of nitrogen supporting export in the oligotrophic subtropical North Pacific Ocean. Limnol. Oceanogr. 47, 1595–1607. https://doi.org/10.4319/lo.2002.47.6.1595.

Druffel, E.R.M., Griffin, S., Witter, A., Nelson, E., Southon, J., Kashgarian, M., Vogel, J., 1995. Gerardia: Bristlecone pine of the deep-sea? Geochim. Cosmochim. Acta 59, 5031–5036. https://doi.org/10.1016/0016-7037(95)00373-8.

Ehrlich, H., Etnoyer, P., Litvinov, S.D., Olennikova, M.M., Domaschke, H., Hanke, T., Born, R., Meissner, H., Worch, H., 2006. Biomaterial structure in deep-sea bamboo coral (Anthozoa: Gorgonacea: Isididae): perspectives for the development of bone implants and templates for tissue engineering. Materwiss. Werksttech. 37, 552–557. https://doi.org/10.1002/mawe.200600036.

Finkel, Z.V., Beardall, J., Flynn, K.J., Quigg, A., Rees, T.A.V., Raven, J.A., 2010. Phytoplankton in a changing world: cell size and elemental stoichiometry. J. Plankton Res. 32, 119–137. https://doi.org/10.1093/plankt/fbp098.

Galbraith, E.D., Kienast, M., Pedersen, T.F., Calvert, S.E., 2004. Glacial-interglacial modulation of the marine nitrogen cycle by high-latitude O_2 supply to the global thermocline. Paleoceanography 19, 1–12. https://doi.org/10.1029/2003PA001000.

Guidi, L., Chaffron, S., Bittner, L., Eveillard, D., Larhlimi, A., Roux, S., Darzi, Y., Audic, S., Berline, L., Brum, J.R., Coelho, L.P., Espinoza, J.C.I., Malviya, S., Sunagawa, S., Dimier, C., Kandels-Lewis, S., Picheral, M., Poulain, J., Searson, S., Stemmann, L., Not, F., Hingamp, P., Speich, S., Follows, M., Karp-Boss, L., Boss, E., Ogata, H., Pesant, S., Weissenbach, J., Wincker, P., Acinas, S.G., Bork, P., De Vargas, C., Iudicone, D., Sullivan, M.B., Raes, J., Karsenti, E., Bowler, C., Gorsky, G., 2016. Plankton networks driving carbon export in the oligotrophic ocean. Nature 532, 465–470. https://doi.org/10.1038/nature16942.

Guilderson, T.P., McCarthy, M.D., Dunbar, R.B., Englebrecht, A., Roark, E.B., 2013. Late Holocene variations in Pacific surface circulation and biogeochemistry inferred from proteinaceous deep-sea corals. Biogeosciences 10, 6019–6028. https://doi.org/10.5194/bg-10-6019-2013.

Jia, G., Li, Z., 2011. Easterly denitrification signal and nitrogen fixation feedback documented in the western Pacific sediments. Geophys. Res. Lett. 38, L24605. https://doi.org/10.1029/2011GL050021. 1–4.

Karl, D., Leteller, R., Tupas, L., Dore, J., Christian, J., Hebel, D., 1997. The role of nitrogen fixation in biogeochemical cycling in the subtropical North Pacific Ocean. Nature 388, 533–538. https://doi.org/10.1038/41474.

Karl, D.M., 1999. Minireviews: A sea of change: biogeochemical variability in the North Pacific Subtropical Gyre. Ecosystems 2, 181–214. https://doi.org/10.1007/s100219900068.

Karl, D.M., Letelier, R., Hebel, D., Tupas, L., Dore, J., Christian, J., Winn, C., 1995. Ecosystem changes in the North Pacific subtropical gyre attributed to the 1991–92 El Niño. Nature 373, 230–234. https://doi.org/10.1038/373230a0.

Karl, D.M., Bidigare, R.R., Letelier, R.M., 2001. Long-term changes in plankton community structure and productivity in the North Pacific Subtropical Gyre: the domain shift hypothesis. Deep-Sea Res., Part 2, Top. Stud. Oceanogr. 48, 1449–1470. https://doi.org/10.1016/S0967-0645(00)00149-1.

Karl, D.M., Church, M.J., Dore, J.E., Letelier, R.M., Mahaffey, C., 2011. Predictable and efficient carbon sequestration in the North Pacific Ocean supported by symbiotic nitrogen fixation. Proc. Natl. Acad. Sci. USA 109 (6), 1842–1849. https://doi.org/10.1073/pnas.1120312109.

Laws, E.A., Popp, B.N., Bidigare, R.R., Kennicutt, M.C., Macko, S.A., 1995. Dependence of phytoplankton carbon isotopic composition on growth rate and $[CO_2]$aq: theoretical considerations and experimental results. Geochim. Cosmochim. Acta 59, 1131–1138. https://doi.org/10.1016/0016-7037(95)00030-4.

Lee, K.E., Slowey, N.C., Herbert, T.D., 2001. Glacial sea surface temperatures in the subtropical North Pacific: a comparison of $U^{k'}_{37}$, $\delta^{18}O$, and foraminiferal assemblage temperature estimates. Paleoceanography 16, 268–279. https://doi.org/10.1029/1999PA000493.

Lu, Z., Liu, Z., Zhu, J., Cobb, K.M., 2018. A review of paleo El Niño-Southern Oscillation. Atmosphere 9 (4), 130. https://doi.org/10.3390/atmos9040130.

Martin, J.H., Knauer, G.A., Karl, D.M., Broenkow, W.W., 1987. VERTEX: carbon cycling in the northeast Pacific. Deep-Sea Res., A, Oceanogr. Res. Pap. 34, 267–285. https://doi.org/10.1016/0198-0149(87)90086-0.

Massana, R., Logares, R., 2013. Eukaryotic versus prokaryotic marine picoplankton ecology. Environ. Microbiol. 15 (5), 1254–1261. https://doi.org/10.1111/1462-2920.12043.

McMahon, K.M., McCarthy, M., Sherwood, O., Larsen, T., Guilderson, T., 2015. Millennial-scale plankton regime shifts in the subtropical North Pacific Ocean. Science 350, 1530–1533. https://doi.org/10.1126/science.aaa9942.

McMahon, K.M., Williams, B., Guilderson, T.P., Glynn, D.S., McCarthy, M.D., 2017. Calibrating amino acid $\delta^{13}C$ and $\delta^{15}N$ offsets between polyp and protein skeleton to develop deep-sea proteinaceous corals as paleoceanographic archives. Geochim. Cosmochim. Acta 220, 261–275. https://doi.org/10.1016/j.gca.2017.09.048.

Monnin, E., Steig, E.J., Siegenthaler, U., Kawamura, K., Schwander, J., Stauffer, B., Stocker, T.F., Morse, D.L., Barnola, J.M., Bellier, B., Raynaud, D., Fischer, H., 2004. Evidence for substantial accumulation rate variability in Antarctica during the Holocene, through synchronization of CO_2 in the Taylor Dome, Dome C and DML ice cores. Earth Planet. Sci. Lett. 224 (1–2), 45–54. https://doi.org/10.1016/j.epsl.2004.05.007.

Moy, C.M., Seltzer, G.O., Rodbell, D.T., Anderson, D.M., 2002. Variability of El Niño Southern Oscillation activity at millennial timescales during the Holocene epoch. Nature 420, 162–165. https://doi.org/10.1038/nature01194.

Pei, Q., Zhang, D.D., Li, J., Lee, H.F., 2017. Proxy-based Northern Hemisphere temperature reconstruction for the Mid-to-Late Holocene. Theor. Appl. Climatol. 130, 1043–1053. https://doi.org/10.1007/s00704-016-1932-5.

Polovina, J.J., Howell, E.A., Abecassis, M., 2008. Ocean's least productive waters are expanding. Geophys. Res. Lett. 35, 2–6. https://doi.org/10.1029/2007GL031745.

Popp, B.N., Laws, E.A., Bidigare, R.R., Dore, J.E., Hanson, K.L., Wakeham, S.G., 1998. Effect of phytoplankton cell geometry on carbon isotopic fractionation. Geochim. Cosmochim. Acta 62, 69–77. https://doi.org/10.1016/S0016-7037(97)00333-5.

Quay, P., Stutsman, J., 2003. Surface layer carbon budget for the subtropical N. Pacific: $\delta^{13}C$ constraints at station ALOHA. Deep-Sea Res., Part 1, Oceanogr. Res. Pap. 50, 1045–1061. https://doi.org/10.1016/S0967-0637(03)00116-X.

Rau, G.H., Takahashi, T., Des Marais, D.J., 1989. Latitudinal variations in plankton $\delta^{13}C$: implications for CO_2 and productivity in past oceans. Nature 341, 516–518. https://doi.org/10.1038/341516a0.

Rau, G.H., Riebesell, U., Wolf-Gladrow, D., 1996. A model of photosynthetic ^{13}C fractionation by marine phytoplankton based on diffusive molecular CO_2 uptake. Mar. Ecol. Prog. Ser. 133, 275–285. https://doi.org/10.3354/meps133275.

Reimer, P.J., Bard, E., Bayliss, A., Beck, J.W., Blackwell, P.G., Ramsey, C.B., Buck, C.E., Cheng, H., Edwards, R.L., Friedrich, M., Grootes, P.M., Guilderson, T.P., Haflidason, H., Hajdas, I., Hatté, C., Heaton, T.J., Hoffmann, D.L., Hogg, A.G., Hughen, K.A., Kaiser, K.F., Kromer, B., Manning, S.W., Niu, M., Reimer, R.W., Richards, D.A., Scott, E.M., Southon, J.R., Staff, R.A., Turney, C.S.M., van der Plicht, J., 2013. IntCal13 and Marine13 radiocarbon age calibration curves 0–50,000 years cal BP. Radiocarbon 55, 1869–1887. https://doi.org/10.2458/azu_js_rc.55.16947.

Roark, E.B., Guilderson, T.P., Dunbar, R.B., Fallon, S.J., Mucciarone, D.A., 2009. Extreme longevity in proteinaceous deep-sea corals. Proc. Natl. Acad. Sci. USA 106, 5204–5208. https://doi.org/10.1073/pnas.0810875106.

Rodionov, S.N., 2004. A sequential algorithm for testing climate regime shifts. Geophys. Res. Lett. 31. https://doi.org/10.1029/2004GL019448. Regime shift program available at: https://www.beringclimate.noaa.gov/regimes/.

Schiff, J.T., Batista, F.C., Sherwood, O.A., Guilderson, T.P., Hill, T.M., Ravelo, A.C., McMahon, K.W., Mccarthy, M.D., 2014. Compound specific amino acid δ^{13}C patterns in a deep-sea proteinaceous coral: implications for reconstructing detailed δ^{13}C records of exported primary production. Mar. Chem. 166, 82–91. https://doi.org/10.1016/j.marchem.2014.09.008.

Schneider, T., Bischoff, T., Haug, G.H., 2014. Migrations and dynamics of the intertropical convergence zone. Nature 513, 45–53. https://doi.org/10.1038/nature13636.

Scott, K.M., Henn-Sax, M., Harmer, T.L., Longo, D.L., Frame, C.H., Cavanaugh, C.M., 2007. Kinetic isotope effect and biochemical characterization of form IA RubisCO from the marine cyanobacterium Prochlorococcus marinus MIT9313. Limnol. Oceanogr. 52, 2199–2204. https://doi.org/10.4319/lo.2007.52.5.2199.

Sherwood, O.A., Scott, D.B., Risk, M.J., 2006. Late Holocene radiocarbon and aspartic acid racemization dating of deep-sea octocorals. Geochim. Cosmochim. Acta 70, 2806–2814. https://doi.org/10.1016/j.gca.2006.03.011.

Sherwood, O.A., Guilderson, T.P., Batista, F.C., Schiff, J.T., McCarthy, M.D., 2014. Increasing subtropical North Pacific Ocean nitrogen fixation since the Little Ice Age. Nature 505, 78–81. https://doi.org/10.1038/nature12784.

Sigman, D.M., DiFiore, P.J., Hain, M.P., Deutsch, C., Karl, D.M., Bo, V., 2009. Sinking organic matter spreads the nitrogen isotope signal of pelagic denitrification in the North Pacific. Geophys. Res. Lett. 36, L08605. https://doi.org/10.1029/2008GL035784. 1–5.

Tesdal, J.E., Galbraith, E.D., Kienast, M., 2013. Nitrogen isotopes in bulk marine sediment: linking seafloor observations with subseafloor records. Biogeosciences 10, 101–118. https://doi.org/10.5194/bg-10-101-2013.

Young, J.N., Bruggeman, J., Rickaby, R.E.M., Erez, J., Conte, M., 2013. Evidence for changes in carbon isotopic fractionation by phytoplankton between 1960 and 2010. Glob. Biogeochem. Cycles 27, 505–515. https://doi.org/10.1002/gbc.20045.

Zubkov, M.V., 2014. Faster growth of the major prokaryotic versus eukaryotic CO_2 fixers in the oligotrophic ocean. Nat. Commun. 5, 1–6. https://doi.org/10.1038/ncomms4776.